JCI insight

Therapeutic suppression of pulmonary neutrophilia and allergic airway hyperresponsiveness by an RORγt inverse agonist

Gregory S. Whitehead, … , Anton M. Jetten, Donald N. Cook

JCI Insight. 2019;4(14):e125528. https://doi.org/10.1172/jci.insight.125528.

Research Article | Inflammation | Therapeutics

Graphical abstract

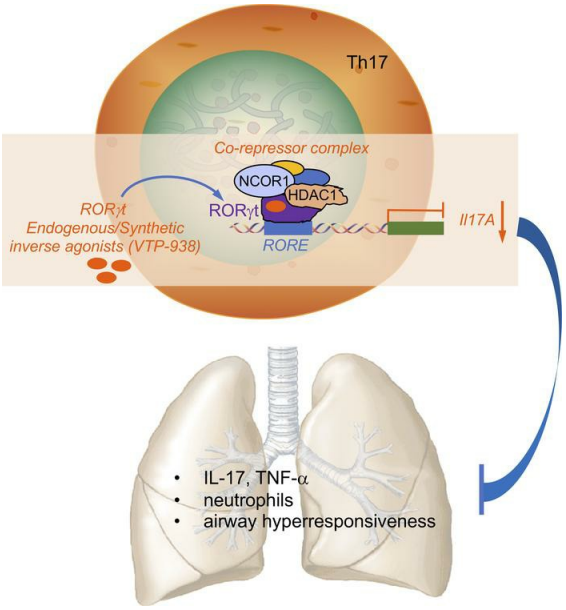

JCI insight

RESEARCH ARTICLE

Therapeutic suppression of pulmonary neutrophilia and allergic airway hyperresponsiveness by an RORγt inverse agonist

Gregory S. Whitehead,[1] Hong Soon Kang,[1] Seddon Y. Thomas,[1] Alexander Medvedev,[2] Tadeusz P. Karcz,[1] Gentaro Izumi,[1] Keiko Nakano,[1] Sergei S. Makarov,[2] Hideki Nakano,[1] Anton M. Jetten,[1] and Donald N. Cook[1]

[1]Immunity, Inflammation, and Disease Laboratory, National Institute of Environmental Health Sciences, NIH, Research Triangle Park, North Carolina, USA. [2]Attagene Inc., Morrisville, North Carolina, USA.

Airway neutrophilia occurs in approximately 50% of patients with asthma and is associated with particularly severe disease. Unfortunately, this form of asthma is usually refractory to corticosteroid treatment, and there is an unmet need for new therapies. Pulmonary neutrophilic inflammation is associated with Th17 cells, whose differentiation is controlled by the nuclear receptor retinoic acid–related orphan receptor γt (RORγt). Here, we tested whether VTP-938, a selective inverse agonist of this receptor, can reduce disease parameters in animal models of neutrophilic asthma. When administered before allergic sensitization through the airway, the RORγt inverse agonist blunted allergen-specific Th17 cell development in lung-draining lymph nodes and attenuated allergen-induced production of IL-17. VTP-938 also reduced pulmonary production of IL-17 and airway neutrophilia when given during the allergen challenge of the model. Finally, in an environmentally relevant model of allergic responses to house dust extracts, VTP-938 suppressed production of IL-17 and neutrophilic inflammation and also markedly diminished airway hyperresponsiveness. Together, these findings suggest that orally available inverse agonists of RORγt might provide an effective therapy to treat glucocorticoid-resistant neutrophilic asthma.

Introduction

Allergic asthma is a chronic inflammatory disease of the airways characterized by reversible airway obstruction, bronchial hyperresponsiveness, and inflammation (1). Recent estimates suggest that approximately 8.4% of the US population is affected by asthma and that health expenditures for adults with this disease reach $18 billion annually (2). Although asthma was once regarded as a single disease, it is now seen as a heterogeneous set of lung pathologies that differ by the extent and nature of airway inflammation, degree of impaired lung function, and response to standard treatment with inhaled glucocorticoids (3). It is likely that different forms of asthma reflect different endotypes (4), subtypes of disease that arise from perturbations of distinct molecular and cellular pathways. The mechanistic basis for discrete endotypes is only beginning to be understood, but observable phenotypes have nonetheless proved useful for predicting responsiveness to specific therapies. For example, patients with eosinophilic airway inflammation generally respond well to corticosteroids (5) and to monoclonal antibodies directed against type 2 cytokines, such as IL-5 (6). However, approximately half of patients with asthma have a noneosinophilic form of this disease, often with neutrophilic inflammation of the airway (7, 8). Cluster analysis of asthmatic phenotypes has revealed that these patients are poorly responsive to inhaled corticosteroids (9) and have particularly severe disease (10). Indeed, steroids might actually exacerbate disease in these patients by inhibiting neutrophil apoptosis (11). Together, these observations underscore the need to accurately identify specific endotypes in asthma and to develop effective therapies that selectively target each form of the disease.

Emerging evidence suggests that some forms of asthma arise in part from the activity of Th17 cells. These cells are controlled largely by the actions of retinoic acid–related orphan receptor γt (RORγt; ref. 12), the isoform of the *Rorc* gene expressed in T cells (13), and mice lacking this transcription factor are

Authorship note: DNC and AMJ contributed equally to this work.

Conflict of interest: SM and AM are shareholders and full time employees of Attagene, Inc.

Submitted: October 12, 2018
Accepted: June 5, 2019
Published: July 25, 2019.

Reference information: *JCI Insight*. 2019;4(14):e125528. https://doi.org/10.1172/jci.insight.125528.

protected against several inflammatory diseases, including allergen-induced lung inflammation (14–16). IL-17 likely contributes to asthma by triggering the secretion of chemokines that recruit neutrophils to the airways, where they promote airway hyperresponsiveness (AHR; refs. 17–19). IL-17 can also enhance AHR by directly binding smooth muscle cells and augmenting their contractility (20). Intriguingly, Th17 cells are steroid resistant (21), suggesting they might be largely responsible for the steroid resistance seen with neutrophilic asthma. Thus, whereas mice overexpressing the Th2 master transcription factor, GATA-3, develop steroid-sensitive airway disease after sensitization and challenge with ovalbumin (OVA), mice that overexpress RORγ develop steroid-resistant disease (22). In view of the central role for RORγt in the development of Th17 cells, we reasoned that nonsteroidal therapies that target this transcription factor might be an effective means to control the development and actions of Th17 cells in asthma.

The discovery that RORs function as ligand-dependent transcription factors launched a search for RORγ inverse agonists that might alleviate Th17-dependent inflammation (23). Inverse agonists of RORγ have subsequently been shown to alleviate Th17-dependent inflammation in several experimental autoimmune disease models in rodents (23–25), and recent studies showed statistically significant efficacy of RORγt inverse agonists in skin explants from patients with psoriasis in phase I and II clinical trials (26). However, we believe the effect of inverse agonists of RORγ on allergen-induced lung inflammation has not been studied. Here, we report that an orally available, selective RORγ inverse agonist, VTP-938, not only attenuates Th17 development and reduces neutrophilic inflammation of the airway but also diminishes AHR in an environmentally relevant, house dust extract–mediated (HDE-mediated) model of asthma. The observations suggest that targeting RORγ might provide a novel strategy in the management of neutrophilic asthma.

Results

VTP-938 selectively inhibits RORγt-dependent transcriptional activation in a dose-dependent manner. The structure of the thiazolopyrrolidine-containing RORγ inverse agonist, VTP-938, is shown in Figure 1A. To confirm that this compound is specific for RORγ, we used factorial reporter technology, which allows simultaneous and quantitative assessment of multiple nuclear receptor activities in transfected cells (27, 28). Of the 24 nuclear receptors tested, RORγ was the only one whose activity was significantly inhibited by VTP-938 at 1.1 μM (Figure 1B). Similar results were obtained at VTP-938 concentrations of 0.37 μM and 10 μM (Supplemental Figure 1, A and B; supplemental material available online with this article; https://doi.org/10.1172/jci.insight.125528DS1). Several previously described inverse agonists of RORγ have displayed activity against other nuclear receptors, including liver X receptor α (LXRα), LXRβ, and pregnane X receptor (PXR) (reviewed in ref. 29). However, VTP-938 did not affect activation of LXRα, PXR, or LXRβ by the LXR agonist T0901317 or the activation of PPARα, PPARβ, or PPARγ by the PPAR agonist GW0742 (Supplemental Figure 1, C and D). VTP-938 inhibited RORγ activity in a dose-dependent manner with an IC_{50} of 0.9 nM (Figure 1C) and selectively inhibited RORγ but not RORα or RORβ (Figure 1D). The selective inhibition of RORγ-dependent transcriptional activity was also seen in CHO Tet-On G3 cells containing a luciferase reporter gene under the control of 5 copies of the ROR response element (RORE) and a doxycycline-inducible (DOX-inducible) RORα or RORγ. Treatment with DOX induced RORα- and RORγ-mediated activation of the luciferase reporter; the activation by RORγ was inhibited by VTP-938 in a dose-dependent manner, whereas RORα-mediated transactivation was unaffected (Supplemental Figure 1, E and F). Mammalian 2-hybrid analysis was used to examine the effect of VTP-938 on the interaction of the RORγ ligand binding domain, termed "RORγ (LBD)," with an LXXLL interaction motif that mediates the binding of coactivators with nuclear receptors. A similar approach was used to study the interaction of RORγ (LBD) with the corepressor nuclear receptor corepressor 1 (NCOR1). An inverse agonist would be predicted to inhibit the interaction of the RORγ (LBD) with the LXXLL coactivator motif and promote interaction with the corepressor (29). Our analyses demonstrated that VTP-938 did indeed inhibit the interaction of the activated RORγ (LBD) with the LXXLL coactivator peptide (Figure 1E) and stimulate its interaction with the corepressor NCOR1 in a dose-dependent manner (Figure 1F), confirming that VTP-938 acts as an inverse agonist. In addition, VTP-938 repressed the activation of the human *IL17* promoter, an established RORγ target gene, in a LUC reporter assay (Figure 1G). Finally, VTP-938 was tested for its ability to block Th17 differentiation in vitro using naive T cells from OVA-specific, *Il17a* fate-mapping mice in which the red fluorescent protein, tdTomato, marks cells that have expressed IL-17 at any time during their development (30). When added throughout the culture, VTP-938 strongly inhibited Th17 cell ($Tomato^+$) development without affecting T cell proliferation (Figure 1H). When the addition of VTP-938 was delayed until day 3 of the culture, the inhibitor

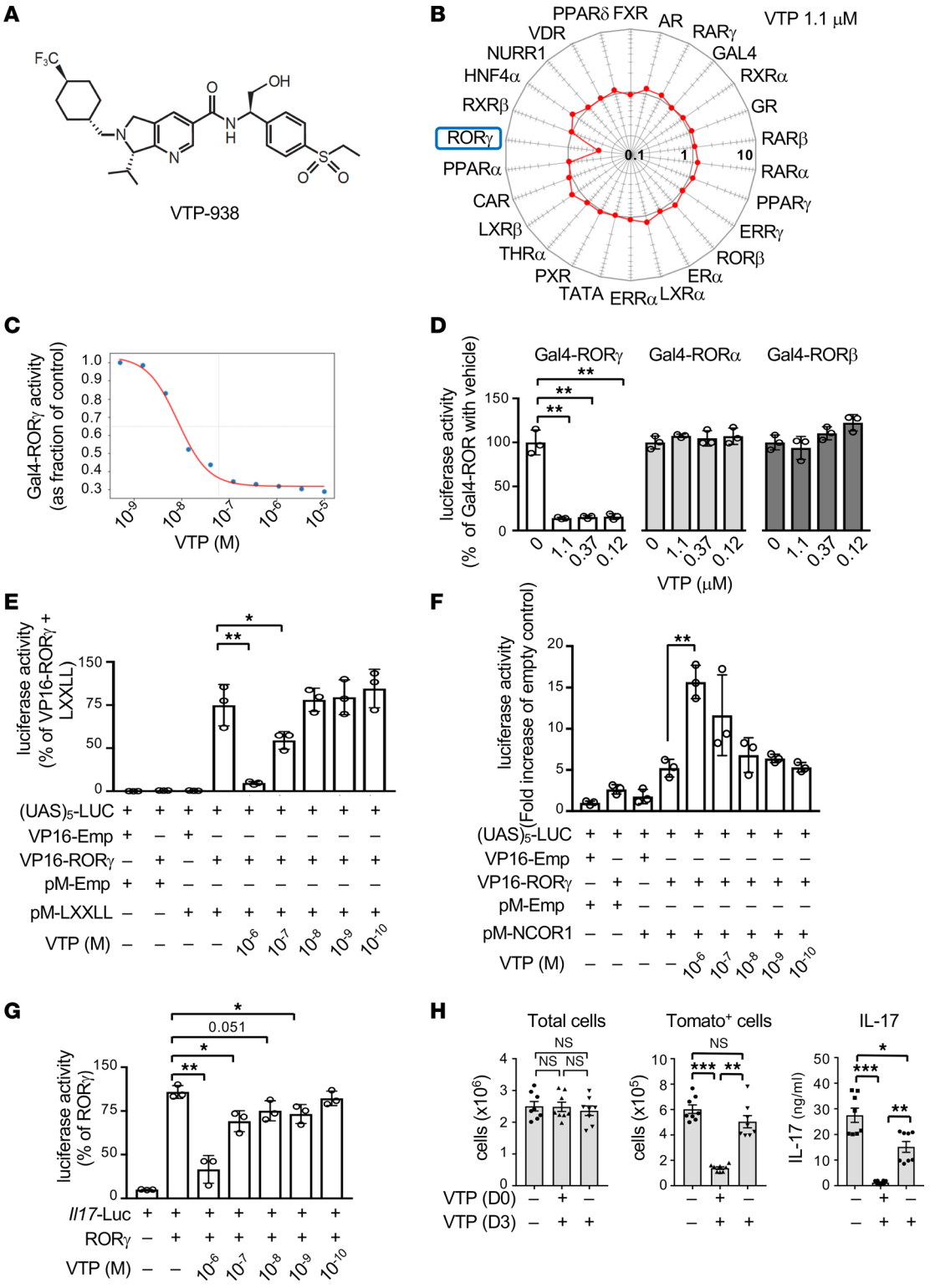

Figure 1. Selective and dose-dependent inhibition of RORγ activity by VTP-938 in vitro. (**A**) Chemical structure of VTP-938 (VTP). (**B**) Trans-FACTORIAL assay showing the effect of VTP (1.1 μM) on the activity of 24 human nuclear receptors in HepG2 cells. Red dots represent relative activity for each receptor in the presence and absence of VTP. "1" indicates VTP has no effect; "10," 10-fold increase; and "0.1," 10-fold decrease. (**C**) Trans-FACTORIAL assay showing the VTP dose–dependent inhibition of RORγ activity. (**D**) Effect of VTP on RORα-, RORβ-, and RORγ-mediated activation of the reporter. (**E**) Effect of VTP on the interaction of the RORγ (LBD) with coactivator nuclear receptor interaction motif LXXLL by mammalian 2-hybrid analysis with $(UAS)_5$-LUC, VP16–RORγ (LBD), and pM-LXXLL. Shown is percentage of $(UAS)_5$-driven LUC activity relative to cells transfected with VP16-RORγ and pM-LXXLL and treated with vehicle (DMSO) (bar 4). Emp, empty vector. LUC, luciferase. (**F**) Analysis of the effect of VTP on the interaction of RORγ (LBD) with corepressor NCOR1 by mammalian 2-hybrid analysis with $(UAS)_5$-LUC, VP16-RORγ (LBD), and pM-NCOR1. Values represent fold increase compared with empty vector control (first bar). Experiments shown in **B**–**F** were done once with triplicate samples and *P* values determined by 2-way ANOVA.

(**G**) VTP inhibition of RORγ-dependent activation of the LUC reporter under transcriptional control of the human *IL17* promoter. Shown is percentage of LUC activity relative to cells transfected with RORγ plus vehicle (DMSO) alone. Data shown represent triplicate samples from a single experiment, representative of 2. *P* values were determined using 2-way ANOVA. (**H**) Effect of VTP when added to Th17 induction cultures at day 0 (D0) or day 3 (D3). Shown are total number of live cells (left), number of Th17 (Tomato$^+$) cells (middle), and IL-17 production (right). Data shown are combined from 2 individual experiments. $^*P < 0.05$, $^{**}P < 0.01$, and $^{***}P < 0.001$, as determined by Kruskal-Wallis 1-way ANOVA with Dunn's multiple-comparisons test.

was no longer able to prevent Th17 cell differentiation but could nonetheless inhibit IL-17 production by those cells. Together, these data show that VTP-938 functions as a selective and effective inverse agonist of RORγ that inhibits IL-17 production by Th17 cells in vitro by repressing activation of the *IL17* promoter, consistent with previous reports that RORγt directly regulates *IL17* transcription (16, 31).

VTP-938 inhibits Th17 cell development in lung-draining lymph nodes. Having established that VTP-938 effectively blocks RORγ function in cultured cells, we next tested whether oral dosing of mice with VTP-938 during the allergic sensitization phase can inhibit the development of allergen-specific Th17 cells in vivo. T cells from B6.Cg-Tg(TcraTcrb)425Cbn/J (OT-II) mice bearing a T cell receptor specific for OVA were adoptively transferred into C57BL/6 mice, which were then sensitized by oropharyngeal (o.p.) instillations of OVA together with the Th17-promoting bacterial product, LPS (19). Lung-draining mediastinal lymph nodes (mLNs) were collected 4 days later and minced and the cells cultured with OVA (Figure 2A). Analysis of cytokines in the supernatants of these cultures revealed that mLNs of mice that had been orally dosed with VTP-938 before sensitization contained significantly less IL-17 than did those of mice treated with the vehicle alone (Figure 2B). IL-4 was slightly increased in cultures derived from VTP-938–treated mice, and IL-5 and IL-13 trended higher, possibly because of a skewing effect of the decreased Th17 differentiation.

Although Th17 cells are a major source of IL-17, it can also be produced by several other cell types, including γδ T cells, macrophages, and neutrophils. To confirm that VTP-938 was acting on naive T cells to prevent their differentiation to Th17 cells in vivo, we again took advantage of the OVA-specific, *Il17a* fate-mapping mice. Donor T cells from these animals were adoptively transferred into C57BL/6 mice, which were then sensitized with OVA alone or OVA/LPS. Flow cytometric analysis of CD4$^+$ T cells (Supplemental Figure 2) from mLNs of the sensitized recipient mice confirmed that the accumulation of OVA-specific, CD4$^+$Tomato$^+$ Th17 cells was dependent on inclusion of the adjuvant, LPS, during allergic sensitization (Figure 2, C and D). The numbers of these cells, as well as their percentages within the CD4$^+$ gate, were markedly diminished in animals receiving VTP-938 before sensitization compared with mice receiving vehicle alone. Together, these data show that oral administration of VTP-938 before sensitization strongly inhibits development of allergen-specific Th17 cells in lung-draining mLNs.

VTP-938 administration during the sensitization phase reduces IL-17 production and airway inflammation in an animal model of asthma. The reduced numbers of Th17 cells in mLNs of mice given VTP-938 during sensitization suggested these animals might also have fewer OVA-specific Th17 cells and less IL-17 in the lung following allergen challenge. To test this, we sensitized mice through the airway with OVA/LPS on 2 occasions and challenged them with aerosolized OVA 1 week after the second sensitization (Figure 3A). Intracellular staining of T cells from lungs of mice that had received VTP-938 during sensitization revealed that these mice had fewer CD4$^+$ cells within the IL-17$^+$ gate than did lungs of mice that had received vehicle alone (Figure 3B). Moreover, single-positive Th17 cells from VTP-938–treated mice had a lower mean fluorescence intensity (MFI) for IL-17 than Th17 cells from vehicle-treated mice (Figure 3C). This suggests not only that VTP-938 inhibits Th17 development in regional lymph nodes (LNs) but also that the Th17 cells that are able to develop in the presence of the inhibitor are less pathogenic, at least as measured by intracellular IL-17. In agreement with these observations, administration of VTP-938 during sensitization led to reduced amounts of extracellular IL-17 in bronchoalveolar lavage fluid (BALF) following OVA challenge (Figure 3D). In contrast, VTP-938 had little effect on intracellular IL-5, IL-13, or IFN-γ in CD4$^+$ T cells (Figure 3, B and C) or on amounts of these cytokines in BALF (Figure 3D).

The pathologic properties of Th17 cells are well described in many disease settings, but these cells can also be nonpathogenic. The differences between pathogenic and nonpathogenic Th17 cells are not well understood but are due in part to levels of GM-CSF (32, 33) and TNF (34). We therefore measured concentrations of these cytokines in BALF of mice that had been treated with VTP-938 before challenge. Although administration of VTP-938 during sensitization did not affect the amount of airway GM-CSF following allergen challenge (data not shown), TNF was significantly reduced (Figure 3D).

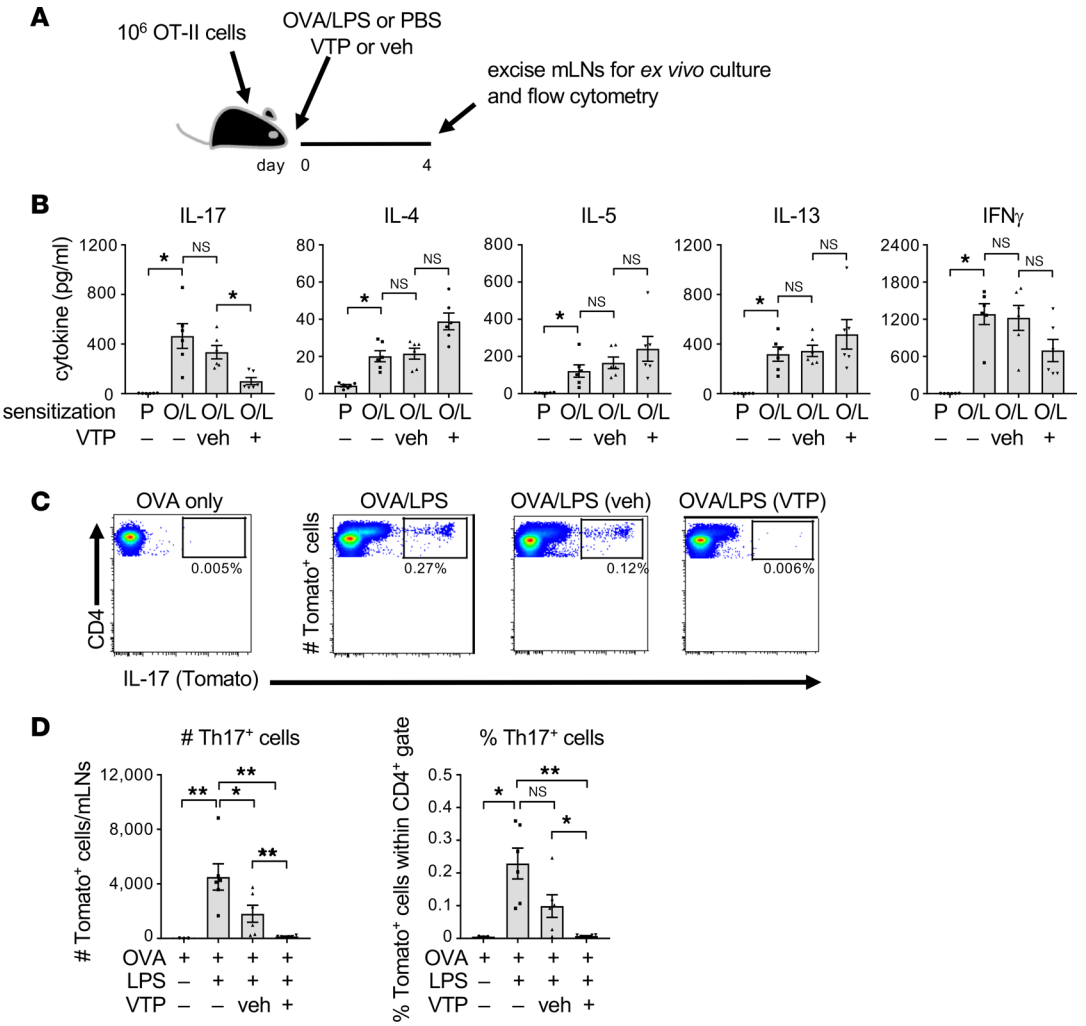

Figure 2. Effect of VTP on developing Th17 responses in regional mLNs. (**A**) Timeline for adoptive cell transfer, VTP administration, allergic sensitization, and analysis of cytokine production in cultures of cells from mLNs. (**B**) Cytokine concentrations in OVA-stimulated cultures of LNs from mice sensitized using OVA/LPS (O/L) or PBS (P) and given VTP or vehicle alone (veh). *n* = 6/group. (**C** and **D**) Analysis of IL-17A fate-mapping cells in mLNs. (**C**) Gating strategy for Th17 (Tomato$^+$) cells within a CD4$^+$ gate. (**D**) Total numbers (left) and percentages (right) of Tomato$^+$ CD4$^+$ cells in mLNs. *n* = 6/group. Data shown represent mean ± SEM from single experiments, each representative of 2. $^*P < 0.05$, and $^{**}P < 0.01$, as determined by Kruskal-Wallis 1-way ANOVA with Dunn's multiple-comparisons test.

VTP-938 therapeutically inhibits established Th17 cells in vivo. Our findings thus far indicated that VTP-938 could suppress the development of Th17 cells during allergic sensitization. However, individuals with neutrophilic asthma have already been sensitized and need therapies that can reduce the severity of exacerbations. We therefore addressed the critical question of whether VTP-938 can also inhibit the actions of Th17 cells that have already developed after sensitization. Mice were sensitized twice by instillations of OVA/LPS to generate allergen-specific T cells and then given either VTP-938 or vehicle during the challenge phase (Figure 4A). Therapeutic treatment with VTP-938 strongly reduced IL-17 levels in BALF, compared with treatment with vehicle alone (Figure 4B), but had no statistically significant effects on IL-5, IL-13, and IFN-γ. Importantly, VTP-938 also strongly reduced the amounts of TNF in the airway. Analysis by mass cytometry (CyTOF) using a custom panel of antibodies revealed that most IL-17–containing cells were conventional T cell receptor αβ–positive (TCRαβ$^+$) Th17 cells, as determined by their staining for CD3, CD4, and RORγ (Figure 4C, Supplemental Table 1, and Supplemental Figure 3). γδ TCR T cells were also detected by CyTOF, and some of these cells contained RORγt, but IL-17 was low upon staining. Using the more sensitive technique of conventional flow cytometry, we were able to identify IL-17$^+$ γδ TCR T cells, albeit fewer in number than IL-17$^+$ αβ TCR T cells. VTP-938 also slightly reduced IL-17 MFI in these cells (Supplemental Figure 4). ILC3s were not detected in this model by either CyTOF or conventional flow cytometry.

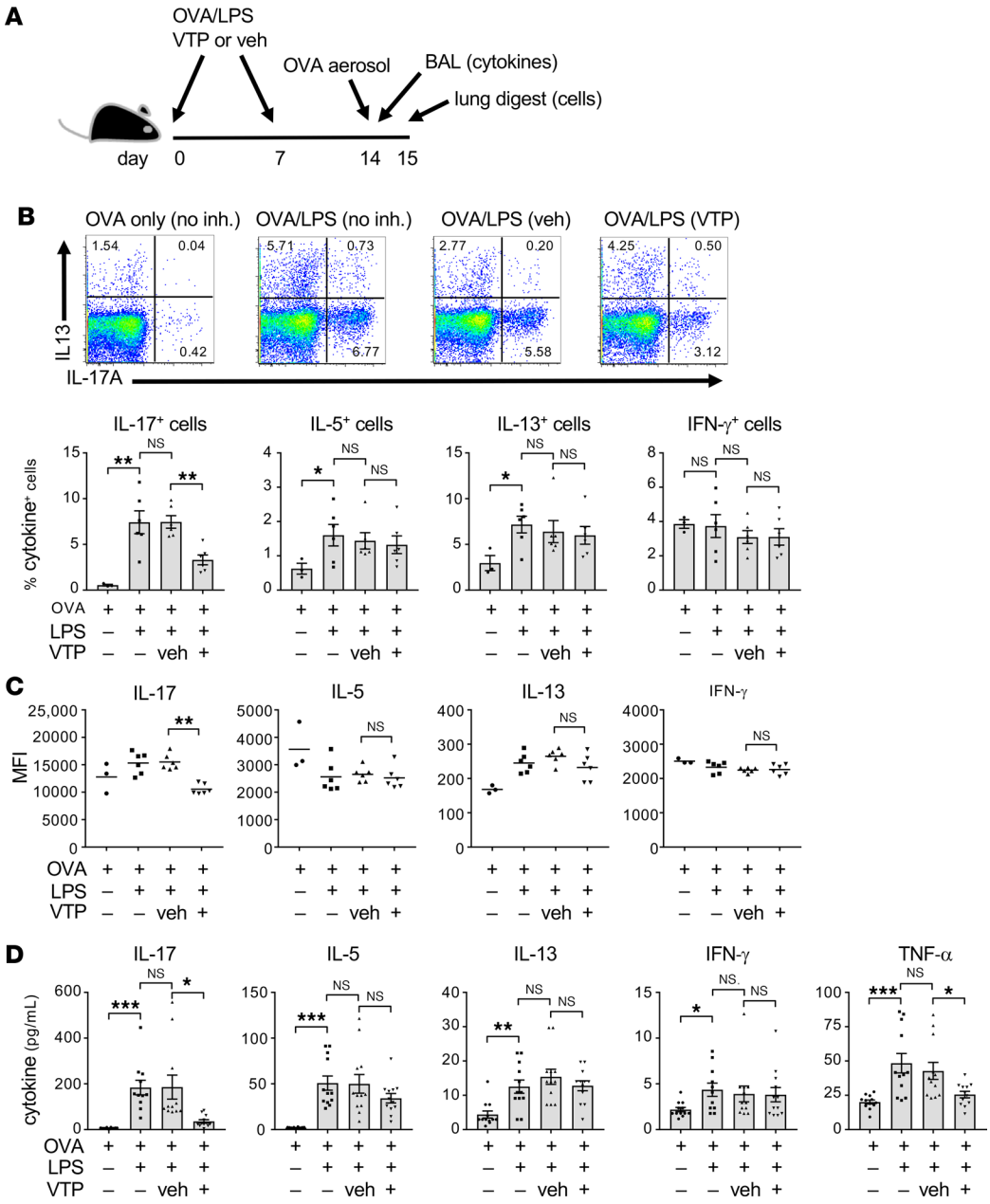

Figure 3. Effect of VTP-938 given during sensitization on airway inflammation following allergen challenge. (**A**) Timeline for VTP-938 (VTP) administration, allergic sensitization, allergen challenge, and lung harvest. (**B**) Analysis of effector T cells in lungs of allergen-challenged mice. Shown are representative cytograms for intracellular staining of IL-17 and IL-13 (top) and bar histograms showing mean percentages ± SEM of cells within a $CD4^+$ T cell gate that stained for the indicated cytokines (bottom). n = 6/group, except OVA-only controls (n = 3/group). (**C**) Mean fluorescence intensity (MFI) staining for the indicated cytokines with a single-positive gate. Data are from a single experiment. n = 6/group, except OVA-only controls (n = 3/group). (**D**) Values represent mean concentrations ± SEM of cytokines in BALF at 4 hours after challenge. n = 12; data are combined from 2 experiments. $^*P < 0.05$, $^{**}P < 0.01$, and $^{***}P < 0.001$, as determined by Kruskal-Wallis 1-way ANOVA with Dunn's multiple-comparisons test.

We next studied mice that received adoptive transfer of OVA-specific, *Il17a* fate-mapping cells before allergic sensitization. Conventional flow cytometry showed that the percentage of fate-mapped Th17 cells that stained for IL-17 was significantly reduced in mice that had received therapeutic VTP-938 compared with those receiving vehicle alone (Figure 4D). These experiments also revealed a relatively small percentage of $IL\text{-}17^+$ cells that were negative for the T cell marker CD3 (Supplemental Figure 4, population P2). The largest population of these cells was $Siglec\text{-}F^{hi}CD88^+$ alveolar macrophages (Supplemental Figure 4, population P5),

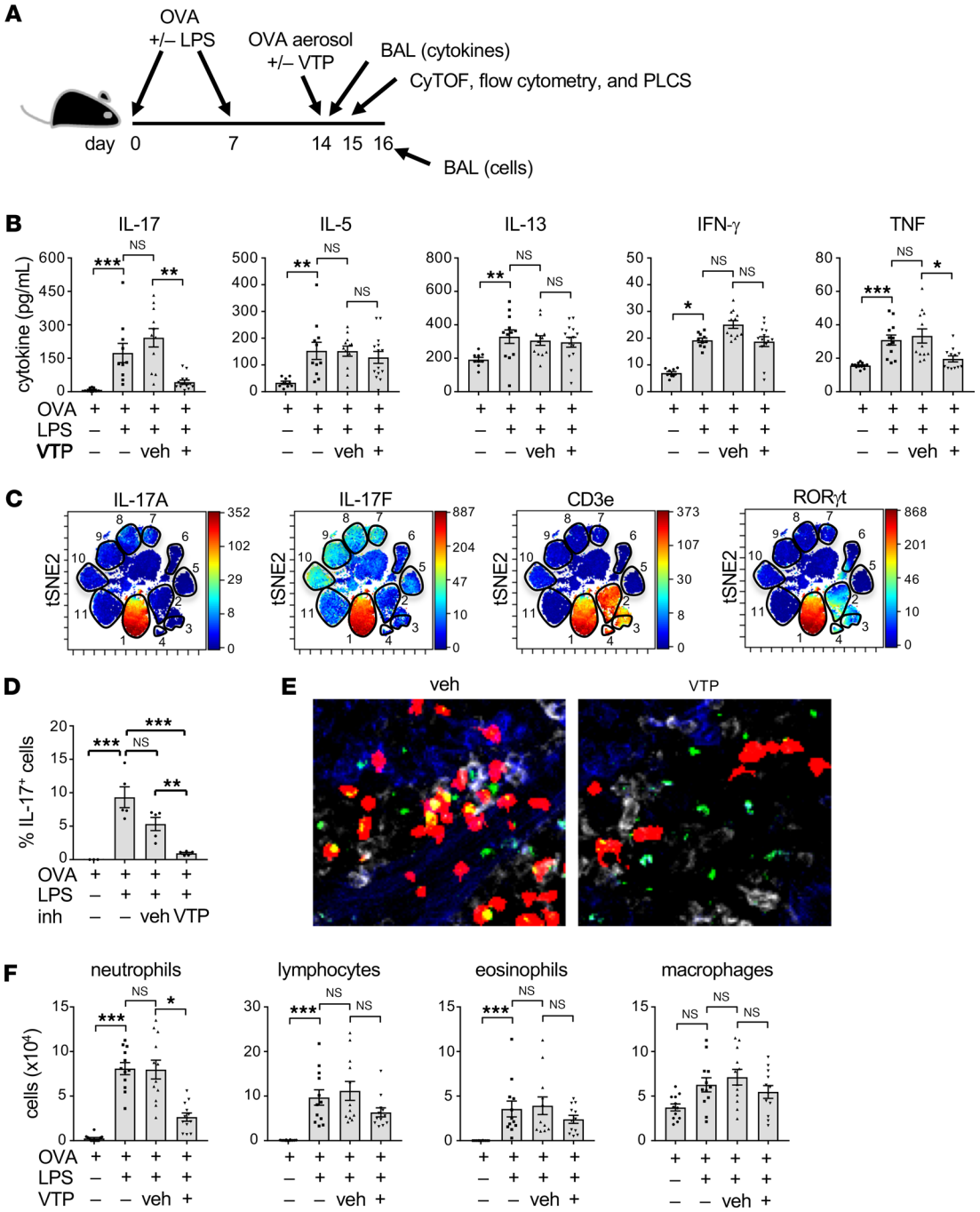

Figure 4. Effect of VTP given before allergen challenge of previously sensitized mice. (**A**) Timeline for OVA/LPS–mediated sensitization of mice given VTP or the vehicle (veh) alone before OVA challenge. PCLS, precision-cut lung slice. (**B**) Mean concentrations ± SEM of cytokines in BALF at 4 hours after allergen challenge. n = 10–12 mice/group; data are combined from 2 experiments. (**C**) CyTOF analysis of lung cells showing the indicated staining for the following populations: 1, Th17 cells; 2, other CD4$^+$ T cells; 3, CD8$^+$ T cells; 4, TCRγδ$^+$ T cells; 5, neutrophils; 6, NK T cells; 7, CD103$^+$ DCs; 8, CD11b$^+$ DCs; 9, interstitial macrophages; 10, alveolar macrophages; and 11, B cells. (**D**) Percentages of IL-17$^+$ cells within a Tomato$^+$ Th17 gate at 24 hours after challenge. (**E**) Confocal image of a PCLS showing Th17 cells (red), IL-17 (green), IL-17–expressing Th17 cells (yellow), CD11c$^+$ antigen-presenting cells (white), and epithelial cells (blue). (**F**) Numbers of cells corresponding to the indicated leukocyte subsets in lung lavages at 48 hours after challenge. Data shown are from a single experiment, representative of 2. n = 6/group. *P < 0.05, and **P < 0.01, as determined by Kruskal-Wallis 1-way ANOVA with Dunn's multiple-comparisons test.

in agreement with a previous report (35). Although VTP-938 significantly reduced amounts of IL-17 in CD4$^+$ T cells, it failed to do so in alveolar macrophages (Supplemental Figure 4). We also performed intracellular staining for IL-17 in PCLSs prepared from mice that had received *Il17a* fate-mapping cells. After OVA challenge, Th17 cells were readily apparent as red fluorescent (Tomato$^+$) cells that localized near airways (Supple-

mental Figure 5). Higher power magnification revealed that many, but not all, of these cells contained IL-17, visible as yellow spots on the red background (Figure 4E). Fate-mapped Th17 cells that received therapeutic VTP-938 appeared to contain less IL-17 than their counterparts in mice receiving vehicle alone. Consistent with its ability to reduce Th17 cell production of IL-17, VTP-938 also reduced neutrophilic inflammation in mice challenged on a single occasion (Figure 4F) or on 3 consecutive days (Supplemental Figure 6). Taken together, these observations demonstrate that VTP-938 can act on established Th17 cells in the lung to inhibit their production of IL-17, thereby attenuating neutrophilic inflammation of the airway.

VTP-938 diminishes asthma-like features in an environmentally relevant model of asthma. Although the OVA/LPS model of asthma is useful for studying the in vivo activity of Th17 cells having a defined allergen specificity, humans do not normally inhale purified preparations of either OVA or LPS. In contrast, most people are routinely exposed to common house dust, which is a complex mixture of substances, including microbial products and indoor allergens (36). To test whether VTP-938 can also attenuate allergic responses to naturally occurring indoor allergens, we sensitized mice to inhaled HDE on days 0 and 7 and challenged the animals on day 14 by administration of the same extract (Figure 5A). The cellular expression of IL-17 in lungs of HDE-challenged mice was very similar to that seen in the OVA/LPS model of asthma, with conventional Th17 cells being the major IL-17–producing cell type (Supplemental Figure 7). Furthermore, mice that were sensitized and challenged with HDE displayed marked increases in IL-17 and type 2 cytokines compared with mice that had been sensitized with HDE but challenged with PBS (Figure 5B). Oral administration of VTP-938 during the HDE challenge phase markedly diminished the amounts of IL-17 in BALF and, in contrast with the OVA/LPS model, reduced type 2 cytokines. As seen in the previous experiments, TNF was also significantly reduced, whereas GM-CSF was not. Analysis of cellular inflammation of the airway revealed that VTP-938 significantly attenuated neutrophilic and lymphocytic inflammation of the airway compared with vehicle alone but had only a minor, statistically insignificant effect on eosinophils (Figure 5C).

AHR is a salient feature of asthma and a major cause of dyspnea. We therefore used invasive measurements of airway resistance to determine whether VTP-938 administration can reduce the severity of this physiologic response to allergen. As expected, mice sensitized and challenged with HDE developed robust AHR, whereas animals challenged with PBS did not (Figure 5D). Mice given VTP-938 during the challenge phase displayed significantly reduced AHR compared with control animals given vehicle alone. Thus, oral administration of VTP-938 can therapeutically reduce the severity of multiple features of asthma, including AHR, in an environmentally relevant model of asthma in which the animals have already been sensitized to allergens.

Discussion

Given the critical role of Th17 cells in multiple inflammatory diseases, including experimental autoimmune encephalomyelitis, collagen-induced arthritis, psoriasis, and allergen-induced airway disease, there has been considerable interest in the development and therapeutic use of molecules that inhibit the actions of these cells. Humanized antibodies against IL-17, IL-17RA, and the p19 subunit of IL-23 have all proved effective in treating psoriasis (37) but thus far have failed to improve symptoms in patients with asthma (ref. 38; https://clinicaltrials.gov/ct2/show/results/NCT01478360?sect=X70156#outcome1). Even if antibodies against 1 or more of these targets eventually prove effective, they will have several inherent drawbacks, including their immunogenicity, their requirement to be injected into the patient, and their high cost of production. In contrast, orally available small molecules that selectively target Th17 cells are nonimmunogenic, convenient to administer, and relatively inexpensive to produce. Because RORγt is required for the development of Th17 cells and for *Il17* expression, identifying inhibitors of this transcription factor has been the focus of considerable investigation, and beginning with the discovery that digoxin is an RORγ antagonist (24), progressively higher affinity antagonists and inverse agonists have been developed and tested in both animals and humans (26). Very recently, orally available inhibitors of RORγt were found to be effective in rodent models of psoriasis (39) and arthritis (40), and recent phase I and phase IIa trials with VTP-43742, an RORγ inverse agonist related to VTP-938, showed statistically significant efficacy in patients with psoriasis (25, 41). These encouraging findings suggest that RORγt inverse agonists might provide a novel therapeutic strategy to treat Th17-dependent inflammatory diseases. However, to our knowledge, small molecule inhibitors of ROR have not been previously tested in an animal model of neutrophilic asthma. Our current work shows that VTP-938 functions as a highly selective ROR inverse agonist that inhibits IL-17 production by repressing the activation of the *IL17* promoter. VTP-938 suppresses Th17 development in regional LNs when given during allergic sensitization but also limits IL-17

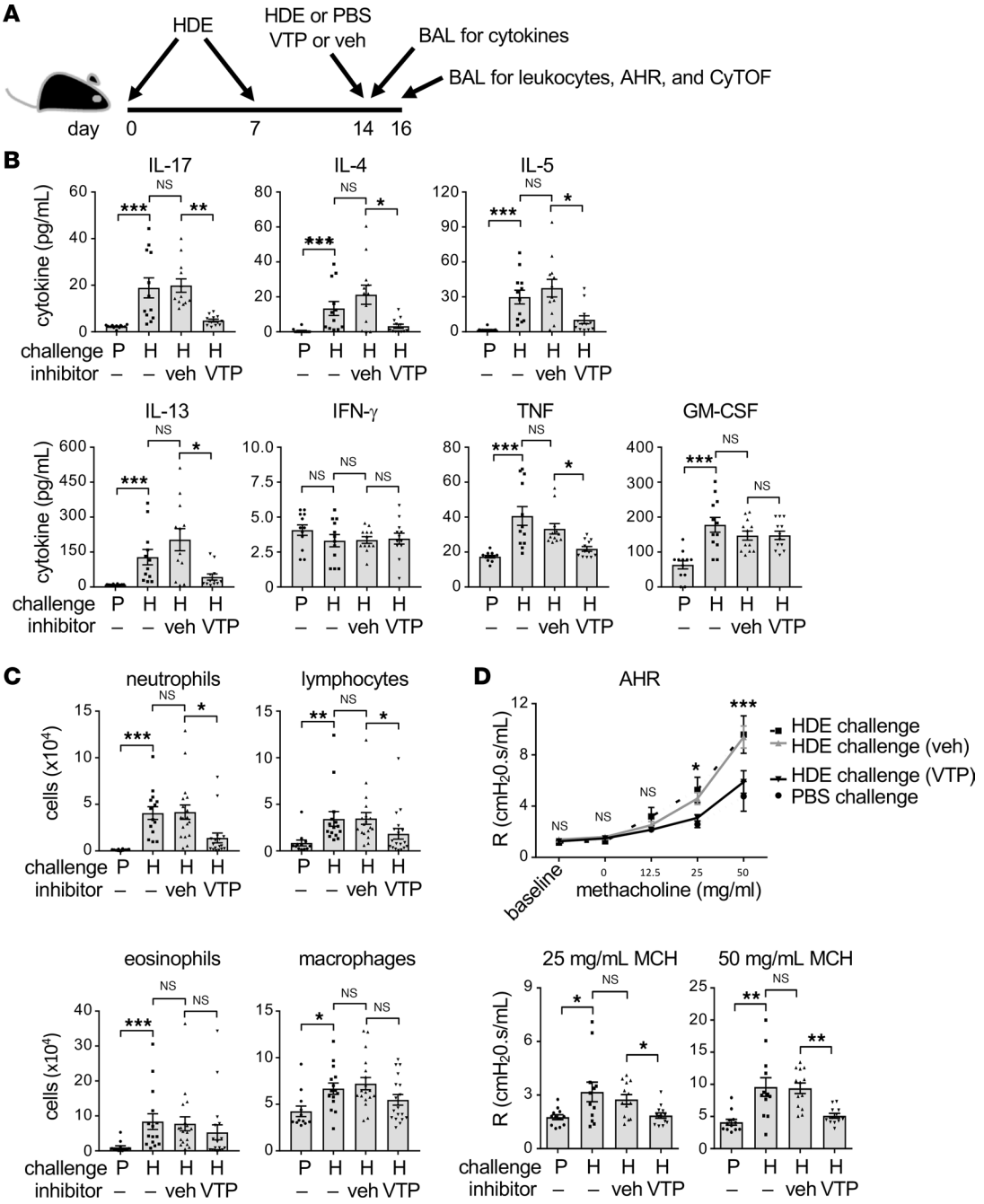

Figure 5. VTP attenuates allergic inflammation and airway hyperresponsiveness in an environmentally relevant model of asthma. (**A**) Timeline for allergic sensitization with HDE and delivery of VTP or vehicle (veh) before challenge with either PBS or HDE. (**B**) Concentrations of cytokines in the airways of mice following challenge with HDE (H) or PBS (P). n = 12 mice/group. (**C**) Total cell numbers for the indicated leukocyte subsets in airways of mice 48 hours after challenge. n = 12 for PBS-treated animals, and n = 15–18 for HDE-treated mice. (**D**) Airway resistance (R) following methacholine challenge of mice previously treated as indicated. n = 6 for PBS challenge, and n = 11–13 for HDE challenge. Data shown are combined from 2 experiments. $^{*}P < 0.05$, $^{**}P < 0.01$, and $^{***}P < 0.001$, as determined by Kruskal-Wallis 1-way ANOVA with Dunn's multiple-comparisons test.

production when given during the challenge phase, a time at which Th17 cells have already developed. Importantly, we also observed that this reduction in IL-17 is associated with reduced neutrophilic inflammation and AHR in an environmentally relevant model of allergic asthma.

In the HDE/OVA model, IL-4 and IL-5 were unexpectedly decreased in the bronchoalveolar lavage of mice treated with VTP-938 immediately before challenge, and eosinophils were reduced in the LPS/OVA model with 3 consecutive OVA challenges. It is established that Foxp3 and RORγt can be simultaneously

expressed in developing T cells, and the ratio of these 2 transcription factors is a major determinant in the ultimate developmental fate of that cell (42). Furthermore, RORγt$^+$ Tregs can effectively suppress Th2 responses (43). The extent to which subtle changes in the ratios of those 2 transcription factors affect the regulatory activity of T cells is unknown, but it is conceivable that in some models of asthma, inhibition of RORγt increases the relative abundance (or activity) of Tregs and that those cells partially suppress type 2 responses, including production of IL-4 and -5 and eosinophilic inflammation. If so, such an increase in Treg activity might be an additional benefit of RORγt inhibition, at least in inflammatory diseases, such as asthma.

As our understanding of the different forms of asthma improves, it will become increasingly feasible to target individual therapies to specific disease endotypes. The factors that predispose to these different endotypes remain poorly understood but likely include both genetic and environmental components. Although RORC polymorphisms have not been extensively studied in the context of human asthma, a recent phenome-wide association study revealed an RORC variant associated with protection from allergies (44). A much larger body of evidence clearly shows that the environment can have a profound influence on the development of immune responses in general (45) and asthma in particular (1). Animal studies are extremely useful in this regard because genes and the environment can both be varied in a controlled manner. For example, different adjuvants can be used during the sensitization phase of asthma models to elicit different forms of disease (46). The HDE model of asthma used in the current study has several advantages, including the use of an environmentally relevant source of allergens and antigens, induction of Th2 and Th17 immunity, mixed neutrophilic and eosinophilic inflammation, and robust airway hyperresponsiveness. These features are reminiscent of severe, steroid-resistant asthma in humans, and our finding that VTP-938 can not only ameliorate neutrophilic inflammation, but also diminish AHR, suggests that orally available inhibitors of RORγt might prove effective in diminishing the severity of exacerbations in a least some patients with neutrophilic asthma. Currently, phenotypic parameters, such as age of onset, blood and sputum eosinophil levels, biomarkers, corticosteroid sensitivity, and extent of obesity are used to infer endotypes (47). It is likely, however, that more accurate assignments of endotypes will eventually be revealed through a combination of noninvasive tests that could include genetic screening, assessments of occupational and domestic exposures, and metabolomics, in addition to T cell lineage–specific cytokines (48). These types of approaches should identify individuals with Th17-dependent exacerbations predicted to be controlled by inverse agonists of RORγt. Although additional studies in this area are clearly needed, our current results provide a proof of principle that inverse agonists of RORγt can provide short-term inhibition of Th17 activity and thereby attenuate neutrophilic inflammation and airway hyperresponsiveness. Finally, given the role of Th17 cells in a variety of other diseases of the lung, including chronic obstructive pulmonary disease (49), hypersensitivity pneumonitis (50), and cystic fibrosis (51, 52), RORγt inverse agonists may provide a novel and effective approach to treat pulmonary inflammation and impaired lung function in a variety of clinical settings.

Methods

Experimental design. Parameters for power calculations were based on data from previous experiments using similar models of asthma. Using an expected effect magnitude of 50%, a standard deviation of 30%, and a power of 90%, we calculated that 6 animals per group would be sufficient for most experiments. In some cases, data were pooled from different experiments to achieve this number. Data collection was never stopped. Before data analysis, a Gaussian distribution analysis was performed using the D'Agostino-Pearson omnibus normality test to determine whether the data fit a normal distribution. If they did, a *t* test or 1-way ANOVA was used. If not, a Mann-Whitney or Kruskal-Wallis test was used. Outliers were identified using the ROUT (robust regression and outlier removal) tool in GraphPad Prism, with Q = 1%. Outliers were removed from the analysis on only 2 occasions: experiments shown in Figure 3D (1 point in the sensitized/no inhibitor group and 1 point in the sensitized/vehicle group) and Figure 5C (1 point in the sensitized/none group and 1 point in the sensitized/VTP group). Selection of endpoints was based on published data and on our own laboratory's previous experience with mouse models of asthma. Experiments were performed a minimum of 2 times, except where indicated. The overall research objective was to determine whether an inhibitor of RORγt can mitigate airway inflammation and other features of asthma in an animal model of neutrophilic asthma. The investigator who performed most of the animal studies was not blinded to their treatment because he dosed the animals with VTP-938 or vehicle and harvested them. However, the investigator who performed all experiments using flow cytometry was blinded to the treatment of the animals, as was the individual who performed the CyTOF experiments.

Animals. Mice were bred and housed in specific pathogen–free conditions at the National Institute of Environmental Health Sciences (NIEHS) and used at between 6 and 12 weeks of age. The following mouse strains were purchased from The Jackson Laboratory: C57BL/6J, OT-II (B6.Cg-Tg[TcraTcrb]425Cbn/J), and B6.Cg-Gt(ROSA)26Sor$^{tm9(CAG-tdTomato)Hze}$/J. The generation and characterization of OVA-specific, *Il17a* fate-mapping mice (B6.Cg-Il17a$^{tm1.1(EYFP/cre)Ehs}$ Gt(ROSA)26Sor$^{tm9(CAG-tdTomato)Hze}$ Tg(TcraTcrb)425Cbn) have been described previously (30). In all experiments, age- and genetically matched mice from the same commercial source were used as controls.

Inverse RORγ agonist. VTP-938 belongs to a group of thiazolopyrrolidine-containing RORγ inverse agonists identified by Vitae Pharmaceuticals, now Allergan Inc. Mass spectrophotometric analysis of VTP-938 in mouse plasma at various times after gavage showed that the in vivo half-life of the compound was approximately 7 hours (Supplemental Figure 8). VTP-938 was administered in vivo at 30 mg/kg by oral gavage in 250 μL vehicle (0.5% natrosol + 1% polysorbate-80) 12 hours and 4 hours before sensitization (or challenge) and 4 hours after sensitization (or challenge).

Mass spectrometric analysis of VTP-938 in mouse plasma. For mass spectrometric analysis, 400 μL ice-cold methanol was added to 100 μL plasma. Samples were vortexed, allowed to precipitate for 10 minutes, and centrifuged at 20,000 RCF for 5 minutes. For liquid chromatography–mass spectrometry analysis, 1 μL of the supernatant was injected onto the column. To generate standard curves, VTP-938 was spiked into mouse plasma. Data were acquired on a Q Exactive Plus mass spectrometer (QE-MS, Thermo Fisher Scientific) interfaced with a Vanquish (Thermo Fisher Scientific) ultra-high–performance liquid chromatography system. Reverse-phase chromatography was performed using a CORTECS C18 column (100 × 2.1 mm i.d., 1.6-μm particle size, Waters Corporation) with solvent A being 5 mM ammonium formate (Sigma) in water (pH 6.5) (18 megohms water from a Picopure 2 system [Hydro Service & Supplies]) and solvent B being methanol (Optima LC/MS grade, Fisher Scientific). The liquid chromatography gradient included a hold at 20% B for the first 2 minutes followed by a ramp from 20% to 95% B from 2 to 7 minutes followed by a 3-minute hold at 95% B. The run was completed with a ramp of 95% to 20% B for 0.5 minutes followed by a 9.5-minute reconditioning at 20% B. The QE-MS was equipped with a HESI source used in the positive ion mode with the following instrument parameters: sheath gas, 40; auxiliary gas, 10; sweep gas, 1; spray voltage, 3.5 kV; capillary temperature, 325°C; S-lens, 50; scan range (*m/z*), 70 to 750; isolation window, 2 *m/z*; resolution: 17,500; automated gain control, 2 × 10e5 ions; and maximum IT, 200 ms. Mass calibration was performed before data acquisition using the LTQ Velos Positive Ion Calibration mixture (Pierce). Data were processed using the Qual Browser application in the Xcalibur software suite (Thermo Fisher Scientific).

Trans-FACTORIAL assays. The activities of 24 nuclear receptors were simultaneously assayed in HepG2 cells using FACTORIAL reporter technology (Attagene, Inc) (27, 28). Twenty-four hours after plating, the transfected cells were supplied with 1% charcoal-stripped FBS (HyClone) and incubated with VTP-938 in the presence or absence of the LXR agonist T0901317 or the PPAR agonist GW0742 for 24 hours. Cell viability was measured in parallel using XTT Cell Proliferation Assay Kit (ATCC). To assess nuclear receptor–specific reporter activity, total RNA was isolated using Invitrogen's PureLink RNA isolation kit, reverse-transcribed into cDNA, and amplified in a single PCR reaction using a pair of common primers. The PCR products were labeled using a 6-FAM–labeled primer and digested with *HpaI* to yield differentially sized, labeled DNA fragments diagnostic of each reporter. The fragments were separated using capillary electrophoresis (CE; Genetic Analyzer 3130xl, ABI), and the relative activities of trans-FACTORIAL endpoints were calculated from the CE electrophoregram peaks using proprietary software (28).

Reporter assays. RORα- and RORγ-dependent transcriptional activity was assessed in vitro using CHO RORα-Tet-On and RORγ-Tet-On cells, respectively, containing DOX-inducible RORα or RORγ (pTRE2-ROR) and a LUC reporter under the transcriptional control of 5 tandem copies of an RORE (pGL4.27-$[RORE]_5$-LUC; refs. 25, 53). Cells were treated with DOX with different concentrations of VTP-938 in DMSO, and ROR-dependent LUC activity was measured 48 hours later in triplicate using a Luciferase Assay Substrate kit (Promega). Mammalian 2-hybrid analysis was used to analyze the effect of VTP-938 on the interaction of the RORγ (LBD) with an LXXLL peptide that mediates either the interaction of coactivators with nuclear receptors or its interaction with the corepressor NCOR1. Briefly, CHO cells were cotransfected with the reporter plasmid pGL4.27-$(UAS)_5$-LUC, containing 5 copies of the Gal4 upstream activating sequence, together with expression plasmids encoding β-galactosidase (pCMV–β-gal), pM-LXXLL encoding the coactivator peptide VESEFPY**LLSLL**GEVSPQP fused to Gal4 (DNA binding domain), and VP16–RORγ (LBD) encoding the RORγ (LBD) fused to the VP16 activation

domain. For analysis of the effect on corepressor interaction, cells were cotransfected with pM-NCOR1 instead of the pM-LXXLL (54). To analyze the effect on the activation of the *IL17* promoter, CHO cells were cotransfected with pCMV–β-gal, pCMV10-3xFlag-RORγ, and a pGL4.14 reporter plasmid under the control of the human *IL17*-3kb-CNS promoter as described (23, 46) and then treated with VTP-938. LUC and β-gal activities were measured 24 hours after treatment using a Luminescent β-galactosidase Detection Kit II (Clontech). All transfections were performed in triplicate and repeated at least twice.

Th17 cell cultures. Naive T cells from *Il17a* fate-mapping mice (30) and DCs from C57BL/6 mice were isolated from spleens of donor animals and cocultured in Th17-promoting conditions with 10 μM $OVA_{323–339}$ peptide as described previously (30). VTP-938 (1 μM) was added at either day 0 or day 3 of culture. tdTomato$^+$ Th17 cells were analyzed by flow cytometry as described previously (30), and IL-17 in culture supernatants was measured by ELISA.

HDEs. Sterile, filtered HDEs were prepared from dust collected from North Carolinian homes as described previously (36). Endotoxin concentration was determined to be 10^{-1} μg LPS/20 μL HDE, as determined by a Limulus Amebocyte Lysate assay (Lonza).

Analysis of Th17 development in regional LNs. Donor cells were prepared from spleens and LNs of either OT-II–transgenic mice or OVA-specific, *Il17a* fate-mapping mice (30); enriched for lymphocytes with a Histopaque 1077 (MilliporeSigma) gradient; and washed 3 times with sterile PBS. Following adoptive transfer of 10^7 donor cells by retro-orbital injection, recipient mice were given oropharyngeal (o.p.) administrations of 100 μg OVA with 100 ng LPS (OVA/LPS) in a total volume of 50 μL. Four days after sensitization, mLNs were excised, minced, pressed through a 70-μm strainer, and cultured at 1×10^6 cells in 200 μL cRPMI media (10% FBS, 0.1% 2-mercaptoethanol, 1 M HEPES, and 1000 IU^{-1} penicillin/streptomycin) containing 10 μg/mL OVA for 2 days. Concentrations of cytokines were measured using a multiplexed fluorescent bead–based immunoassay according to the instructions of the manufacturer (Bio-Rad Laboratories). For some adoptive transfer experiments with OVA-specific, *Il17a* fate-mapping cells, recipient mice were sensitized on 3 consecutive days with OVA/LPS before LN harvest.

Animal models of asthma. For the OVA/LPS model of asthma, mice were lightly anesthetized with isoflurane and given 2 o.p. administrations, 1 week apart, of 50 μg LPS-free OVA (Worthington Biomedical) with 100 ng LPS from *E. coli* 0111:B4 (MilliporeSigma) in a total volume of 50 μL, with PBS as the diluent. Sensitized mice were challenged 1 week after the second sensitization by exposing them to an aerosol of 1% OVA (MilliporeSigma) in PBS on a single occasion for 1 hour, or on 3 consecutive days for 30 minutes. Following euthanasia at 4 hours after challenge, BALF was collected for analysis of cytokines in the airway. Airway inflammation and AHR were assessed at 48 hours after challenge. For the HDE model, animals were sensitized by o.p. administrations of 10 μL HDE on days 0 and 7 and challenged on day 14 with 5 μL of the same extract.

CyTOF. Mice were sensitized to OVA/LPS or HDE as described above but 4 hours before allergen challenge received 250 μg of Brefeldin A (MilliporeSigma) in PBS by i.p. injection. This reagent was also included at 5 ng/mL in all solutions up to the cell permeabilization step. Excised lungs were digested as described previously (55), and 3×10^6 single lung cells were incubated for 5 minutes with 1 μM of Cell-ID Cisplatin (Fluidigm) at room temperature to identify dead cells. Subsequent incubation and wash steps were performed using Maxpar Cell Staining Buffer (Fluidigm). A nonspecific binding-blocking reagent cocktail containing anti–mouse CD16/CD32, normal mouse serum, and rat serum was added, followed by a 30-minute incubation with 50 μL of metal-conjugated antibodies against cell surface proteins (Supplemental Table 1). For some proteins, a fluorescently labeled primary antibody was used, followed by staining with a metal-conjugated secondary antibody. For intracellular staining, 100 μL of IC Fixation Buffer (eBioscience) was added and the cells incubated at RT for 20 minutes. Cells were washed with Permeabilization Buffer (eBioscience) and incubated in 100 μL of Permeabilization Buffer containing antibodies against intracellular proteins for 30 minutes. After another wash step in Permeabilization Buffer, metal-conjugated secondary antibodies (Supplemental Table 1) were added if necessary. Cells were washed with Maxpar Cell Staining Buffer and incubated with 125 nM Cell-ID Intercalator-Ir (Fluidigm) in Maxpar Fix and Perm Buffer (Fluidigm) overnight. On the following day, cells were washed and filtered with a Flowmi tip strainer (Fisher Scientific, Thermo Fisher Scientific). Data were acquired using a Helios mass cytometer (Fluidigm) and analyzed using the Cytobank platform (http://www.cytobank.org/; Cytobank Inc.).

PCLSs. Before sensitization with OVA/LPS, C57BL/6 mice received 10^7 cells from LNs and spleens of OT-II crossed with *Il17a* fate-mapping mice. The animals were euthanized 24 hours after the second OVA challenge, and PLCSs were prepared from excised lungs and stained as described previously (56). Briefly,

the slices were incubated with 50 ng/mL PMA, 500 ng/mL ionomycin (MilliporeSigma), and 0.2 μM Golgi Stop (containing monensin) (BD Bioscience, catalog BD554724) for 4 hours, then stained with antibodies against CD11c and CD324/E-cadherin, followed by permeabilization and intracellular staining for IL-17. Images of the stained slices were captured using a Zeiss 880 multiphoton laser-scanning microscope and analyzed using Zen software (Carl Zeiss).

Lung function testing. Evaluations of AHR were performed as previously described (19), using the FlexiVent mechanical ventilator system (Scireq). A single-compartment model of the lung was used to assess total respiratory system resistance after delivery of aerosolized methacholine using an ultrasonic nebulizer. Data are reported as peak resistance values.

Statistics. Most statistical calculations were performed using GraphPad Prism 7 (GraphPad Software Inc.). Unless stated otherwise, data are shown as mean ± SEM. Differences between groups were identified by ANOVA using Dunn's multiple-comparisons tests. *P* values of less than 0.05 were considered statistically significant.

Study approval. Animal study protocols were approved by the NIEHS Animal Care and Use Committee, in accordance with guidelines provided by the NIH's *Guide for the Care and Use of Laboratory Animals* (National Academies Press, 2011).

Author contributions

AMJ conceived of the project, provided the inverse agonist, and oversaw in vitro experiments. GSW, HSK, SYT, TPK, GI, KN, AM, and SSM performed experiments and analyzed data. HN designed and oversaw CyTOF experiments. DNC and AMJ oversaw experiments, analyzed data, and wrote the manuscript. All authors made editorial suggestions and approved the final version.

Acknowledgments

We thank Leesa Deterding and Jason Williams for mass spectrophometric analysis of VTP-938; Lyubov Medvedeva, Kristen Gorman, and Elena Martsen for factorial analysis of VTP-938; Ligon Perrow for animal colony support; and Michael Fessler and Jennifer Martinez for critical reading of the manuscript. This work was supported by the Intramural Research Program of the NIH, the NIEHS, NIH Z01-ES-101585 (to AJM) and ZIA-ES-102025-09 (to DNC).

Address correspondence to: Anton M. Jetten or Donald N. Cook, 111 T.W. Alexander Drive, Building 101, D264, Research Triangle Park, North Carolina 27709, USA. Phone: 984.287.4094; Email: jetten@niehs.nih.gov (A.M. Jetten). 984.287.4245; Email: cookd@niehs.nih.gov (D.N. Cook).

1. Martinez FD, Vercelli D. Asthma. *Lancet*. 2013;382(9901):1360–1372.
2. Sullivan PW, et al. The relationship between asthma, asthma control and economic outcomes in the United States. *J Asthma*. 2014;51(7):769–778.
3. Moore WC, et al. Clinical heterogeneity in the severe asthma research program. *Ann Am Thorac Soc*. 2013;10(suppl):S118–S124.
4. Anderson GP. Endotyping asthma: new insights into key pathogenic mechanisms in a complex, heterogeneous disease. *Lancet*. 2008;372(9643):1107–1119.
5. Little SA, Chalmers GW, MacLeod KJ, McSharry C, Thomson NC. Non-invasive markers of airway inflammation as predictors of oral steroid responsiveness in asthma. *Thorax*. 2000;55(3):232–234.
6. Pavord ID, et al. Mepolizumab for severe eosinophilic asthma (DREAM): a multicentre, double-blind, placebo-controlled trial. *Lancet*. 2012;380(9842):651–659.
7. McGrath KW, et al. A large subgroup of mild-to-moderate asthma is persistently noneosinophilic. *Am J Respir Crit Care Med*. 2012;185(6):612–619.
8. Thomson NC. Novel approaches to the management of noneosinophilic asthma. *Ther Adv Respir Dis*. 2016;10(3):211–234.
9. Green RH, Brightling CE, Woltmann G, Parker D, Wardlaw AJ, Pavord ID. Analysis of induced sputum in adults with asthma: identification of subgroup with isolated sputum neutrophilia and poor response to inhaled corticosteroids. *Thorax*. 2002;57(10):875–879.
10. Moore WC, et al. Sputum neutrophil counts are associated with more severe asthma phenotypes using cluster analysis. *J Allergy Clin Immunol*. 2014;133(6):1557–63.e5.
11. Wang M, et al. Impaired anti-inflammatory action of glucocorticoid in neutrophil from patients with steroid-resistant asthma. *Respir Res*. 2016;17(1):153.
12. Ivanov, et al. The orphan nuclear receptor RORgammat directs the differentiation program of proinflammatory IL-17$^+$ T helper cells. *Cell*. 2006;126(6):1121–1133.
13. He YW, Deftos ML, Ojala EW, Bevan MJ. RORγt, a novel isoform of an orphan receptor, negatively regulates Fas ligand expression and IL-2 production in T cells. *Immunity*. 1998;9(6):797–806.

14. Cook DN, Kang HS, Jetten AM. Retinoic acid-related orphan receptors (RORs): regulatory functions in immunity, development, circadian rhythm, and metabolism. *Nucl Receptor Res*. 2015;2:101185.
15. Tilley SL, et al. Retinoid-related orphan receptor γ controls immunoglobulin production and Th1/Th2 cytokine balance in the adaptive immune response to allergen. *J Immunol*. 2007;178(5):3208–3218.
16. Yang XO, et al. T helper 17 lineage differentiation is programmed by orphan nuclear receptors RORα and RORγ. *Immunity*. 2008;28(1):29–39.
17. Barczyk A, Pierzchala W, Sozañska E. Interleukin-17 in sputum correlates with airway hyperresponsiveness to methacholine. *Respir Med*. 2003;97(6):726–733.
18. Liang SC, et al. An IL-17F/A heterodimer protein is produced by mouse Th17 cells and induces airway neutrophil recruitment. *J Immunol*. 2007;179(11):7791–7799.
19. Wilson RH, Whitehead GS, Nakano H, Free ME, Kolls JK, Cook DN. Allergic sensitization through the airway primes Th17-dependent neutrophilia and airway hyperresponsiveness. *Am J Respir Crit Care Med*. 2009;180(8):720–730.
20. Kudo M, et al. IL-17A produced by αβ T cells drives airway hyper-responsiveness in mice and enhances mouse and human airway smooth muscle contraction. *Nat Med*. 2012;18(4):547–554.
21. McKinley L, et al. TH17 cells mediate steroid-resistant airway inflammation and airway hyperresponsiveness in mice. *J Immunol*. 2008;181(6):4089–4097.
22. Ano S, et al. Transcription factors GATA-3 and RORγt are important for determining the phenotype of allergic airway inflammation in a murine model of asthma. *J Immunol*. 2013;190(3):1056–1065.
23. Xu T, Wang X, Zhong B, Nurieva RI, Ding S, Dong C. Ursolic acid suppresses interleukin-17 (IL-17) production by selectively antagonizing the function of RORγt protein. *J Biol Chem*. 2011;286(26):22707–22710.
24. Huh JR, et al. Digoxin and its derivatives suppress TH17 cell differentiation by antagonizing RORγt activity. *Nature*. 2011;472(7344):486–490.
25. Smith SH, et al. Development of a topical treatment for psoriasis targeting RORγ: from bench to skin. *PLoS One*. 2016;11(2):e0147979.
26. Jetten AM, Takeda Y, Slominski A, Kang HS. Retinoic acid-related Orphan Receptor γ (RORγ): connecting sterol metabolism to regulation of the immune system and autoimmune disease. *Curr Opin Toxicol*. 2018;8:66–80.
27. Martin MT, et al. Impact of environmental chemicals on key transcription regulators and correlation to toxicity end points within EPA's ToxCast program. *Chem Res Toxicol*. 2010;23(3):578–590.
28. Romanov S, et al. Homogeneous reporter system enables quantitative functional assessment of multiple transcription factors. *Nat Methods*. 2008;5(3):253–260.
29. Mutemberezi V, Guillemot-Legris O, Muccioli GG. Oxysterols: From cholesterol metabolites to key mediators. *Prog Lipid Res*. 2016;64:152–169.
30. Shalaby KH, et al. Pathogenic TH17 inflammation is sustained in the lungs by conventional dendritic cells and Toll-like receptor 4 signaling. *J Allergy Clin Immunol*. 2018;142(4):1229–1242.e6.
31. Wang X, et al. Transcription of Il17 and Il17f is controlled by conserved noncoding sequence 2. *Immunity*. 2012;36(1):23–31.
32. Codarri L, et al. RORγt drives production of the cytokine GM-CSF in helper T cells, which is essential for the effector phase of autoimmune neuroinflammation. *Nat Immunol*. 2011;12(6):560–567.
33. El-Behi M, et al. The encephalitogenicity of T(H)17 cells is dependent on IL-1- and IL-23-induced production of the cytokine GM-CSF. Nat Immunol. 2011;12(6):568–575.
34. Kleinewietfeld M, et al. Sodium chloride drives autoimmune disease by the induction of pathogenic TH17 cells. *Nature*. 2013;496(7446):518–522.
35. Song C, et al. IL-17-producing alveolar macrophages mediate allergic lung inflammation related to asthma. *J Immunol*. 2008;181(9):6117–6124.
36. Wilson RH, et al. The Toll-like receptor 5 ligand flagellin promotes asthma by priming allergic responses to indoor allergens. *Nat Med*. 2012;18(11):1705–1710.
37. Papp KA, et al. Brodalumab, an anti-interleukin-17-receptor antibody for psoriasis. *N Engl J Med*. 2012;366(13):1181–1189.
38. Busse WW, et al. Randomized, double-blind, placebo-controlled study of brodalumab, a human anti-IL-17 receptor monoclonal antibody, in moderate to severe asthma. *Am J Respir Crit Care Med*. 2013;188(11):1294–1302.
39. Takaishi M, Ishizaki M, Suzuki K, Isobe T, Shimozato T, Sano S. Oral administration of a novel RORγt antagonist attenuates psoriasis-like skin lesion of two independent mouse models through neutralization of IL-17. *J Dermatol Sci*. 2017;85(1):12–19.
40. Guendisch U, et al. Pharmacological inhibition of RORγt suppresses the Th17 pathway and alleviates arthritis in vivo. *PLoS One*. 2017;12(11):e0188391.
41. Bronner SM, Zbieg JR, Crawford JJ. RORγ antagonists and inverse agonists: a patent review. *Expert Opin Ther Pat*. 2017;27(1):101–112.
42. Bettelli E, et al. Reciprocal developmental pathways for the generation of pathogenic effector TH17 and regulatory T cells. *Nature*. 2006;441(7090):235–238.
43. Ohnmacht C, et al. Mucosal immunology. The microbiota regulates type 2 immunity through RORγt$^+$ T cells. *Science*. 2015;349(6251):989–993.
44. Ehm MG, et al. Phenome-wide association study using research participants' self-reported data provides insight into the Th17 and IL-17 pathway. *PLoS One*. 2017;12(11):e0186405.
45. Brodin P, Davis MM. Human immune system variation. *Nat Rev Immunol*. 2017;17(1):21–29.
46. Whitehead GS, et al. TNF is required for TLR ligand-mediated but not protease-mediated allergic airway inflammation. *J Clin Invest*. 2017;127(9):3313–3326.
47. Carr TF, Zeki AA, Kraft M. Eosinophilic and Noneosinophilic Asthma. *Am J Respir Crit Care Med*. 2018;197(1):22–37.
48. Turi KN, Romick-Rosendale L, Ryckman KK, Hartert TV. A review of metabolomics approaches their application in identifying causal pathways of childhood asthma. *J Allergy Clin Immunol*. 2018;141(4):1191–1201.
49. Barnes PJ. Inflammatory mechanisms in patients with chronic obstructive pulmonary disease. *J Allergy Clin Immunol*. 2016;138(1):16–27.

50. Simonian PL, et al. Th17-polarized immune response in a murine model of hypersensitivity pneumonitis and lung fibrosis. *J Immunol*. 2009;182(1):657–665.
51. Chan YR, et al. Patients with cystic fibrosis have inducible $IL^{-}17^{+}IL^{-}22^{+}$ memory cells in lung draining lymph nodes. *J Allergy Clin Immunol*. 2013;131(4):1117–1129.e1.
52. Tan HL, Regamey N, Brown S, Bush A, Lloyd CM, Davies JC. The Th17 pathway in cystic fibrosis lung disease. *Am J Respir Crit Care Med*. 2011;184(2):252–258.
53. Slominski AT, et al. RORα and ROR γ are expressed in human skin and serve as receptors for endogenously produced noncalcemic 20-hydroxy- and 20,23-dihydroxyvitamin D. *FASEB J*. 2014;28(7):2775–2789.
54. Kurebayashi S, et al. Selective LXXLL peptides antagonize transcriptional activation by the retinoid-related orphan receptor RORgamma. *Biochem Biophys Res Commun*. 2004;315(4):919–927.
55. Nakano H, et al. Pulmonary CD103(+) dendritic cells prime Th2 responses to inhaled allergens. *Mucosal Immunol*. 2012;5(1):53–65.
56. Lyons-Cohen MR, Thomas SY, Cook DN, Nakano H. Precision-cut mouse lung slices to visualize live pulmonary dendritic cells. *J Vis Exp*. 2017;(122):55465.